Supplement of Atmos. Chem. Phys., 25, 10229–10243, 2025
https://doi.org/10.5194/acp-25-10229-2025-supplement

Atmospheric Chemistry and Physics
Open Access
EGU

Supplement of

Ozonolysis of primary biomass burning organic aerosol particles: insights into reactivity and phase state

Sophie Bogler et al.

Correspondence to: David M. Bell (david.bell@psi.ch)

Contents of this file:

Table S1: Experimental flow settings and O_3 concentrations (part 1/2). The column "step #" numbers the varying ozone conditions set for each experiment; the label "(POA)" denotes steps where the ozone concentration was set to 0 to measure the composition of POA (see the method section of the main manuscript for more details).

Campaign March 2022						
exp #	experiment name (date)	step #	dry air [L/min]	exhaust O_3 [L/min]	O_3 in OFR [L/min]	O_3 conc. [ppm]
1	spruce1 (02.03.2022)	1 (POA)	5.1	0.1	0	0.061 ± 0.007
		2	5	0	0.1	2.318 ± 0.013
		3	5.02	0.02	0.08	1.897± 0.016
		4	5.04	0.04	0.06	1.408± 0.009
		5	5.06	0.06	0.04	0.975± 0.012
		6	5.08	0.08	0.02	0.536± 0.009
		7 (POA)	5.1	0.1	0	0.040± 0.008
		8	5.09	0.09	0.01	0.295± 0.009
		9	5.095	0.095	0.005	0.167± 0.009
		10	5.096	0.096	0.004	0.147± 0.009
		11	5.097	0.097	0.003	0.126± 0.007
		12	5.098	0.098	0.002	0.105± 0.007
		13	5.099	0.099	0.001	0.063± 0.008
		14 (POA)	5.1	0.1	0	0.041± 0.008
2	open1 (04.03.2022)	1 (POA)	5	0.1	0	0.062± 0.007
		2	4.9	0	0.1	2.443± 0.016
		3	4.999	0.099	0.001	0.081± 0.006
		4	4.998	0.098	0.002	0.104± 0.008
		5	4.997	0.097	0.003	0.124± 0.009
		6	4.996	0.096	0.004	0.166± 0.009
		7 (POA)	5	0.1	0	0.040± 0.008
		8	4.99	0.09	0.01	0.340± 0.009
		9	4.993	0.093	0.007	0.253± 0.008
		10	4.98	0.08	0.02	0.628± 0.014
		11	4.96	0.06	0.04	1.192± 0.018
		12 (POA)	5	0.1	0	0.047± 0.014
3	beech1 (09.03.2022)	1 (POA)	4.5	0.1	0	0.059± 0.006
		2	4.4	0	0.1	2.941± 0.040
		3	4.499	0.099	0.001	0.062± 0.008
		4	4.498	0.098	0.002	0.101± 0.006
		5	4.497	0.097	0.003	0.124± 0.009
		6	4.496	0.096	0.004	0.166± 0.007
		7 (POA)	4.5	0.1	0	0.040± 0.006
3		8	4.48	0.08	0.02	0.787± 0.017
		9	4.46	0.06	0.04	1.619± 0.015
		10	4.42	0.02	0.08	3.103± 0.081
		11 (POA)	4.5	0.1	0	0.046± 0.011
4	spruce2 (10.03.2022)	1 (POA)	4.5	0.1	0	-
		2	4.4	0	0.1	3.249± 0.021
		3	4.498	0.098	0.002	0.123± 0.009
		4	4.496	0.096	0.004	0.186± 0.007
		5	4.492	0.092	0.008	0.360± 0.006
		6 (POA)	4.5	0.1	0	0.057± 0.006
		7	4.485	0.085	0.015	0.058± 0.007
		8	4.47	0.07	0.03	0.656± 0.012
		9	4.45	0.05	0.05	1.247± 0.012
		10	4.425	0.025	0.075	1.913± 0.010
		11 (POA)	4.5	0.1	0	0.230± 0.470
5	open2 (11.03.2022)	1 (POA)	4.3	0.1	0	0.041± 0.013
		2	4.2	0	0.1	3.967± 0.409
		3	4.298	0.098	0.002	0.121± 0.008
		4	4.296	0.096	0.004	0.207± 0.007
		5	4.294	0.094	0.006	0.307± 0.015
		6	4.29	0.09	0.01	0.493± 0.007
		7 (POA)	4.3	0.1	0	0.041± 0.009
		8	4.28	0.08	0.02	0.920± 0.016
		9	4.26	0.06	0.04	1.735± 0.009
		10	4.22	0.02	0.08	3.304± 0.020
		11 (POA)	4.3	0.1	0	0.043± 0.010

Table S2: Experimental flow settings and O_3 concentrations (part 2/2). The column "step #" numbers the varying ozone and RH conditions set for each experiment; the label "(POA)" denotes steps where the ozone concentration was set to 0 to measure the composition of POA (see the method section of the main manuscript for more details).

Campaign May 2022									
exp #	experiment name (date)	step #	dry air [L/min]	wet air [L/min]	exhaust O_3 [L/min]	O_3 in OFR [L/min]	O_3 conc. [ppm]	RH level [%]
6	beech2 (16.05.2022)	1 (POA)	5.1	0	0.1	0	0.017± 0.002	-
		2	5.099	0	0.099	0.001	0.025± 0.002	-
		3	5.096	0	0.096	0.004	0.104± 0.002	-
		4	5.094	0	0.094	0.006	0.154± 0.002	-
		5	5.092	0	0.092	0.008	0.216± 0.002	-
		6 (POA)	5.1	0	0.1	0	0.009± 0.002	-
		7	5.075	0	0.075	0.025	0.730± 0.002	-
		8	5.05	0	0.05	0.05	1.460± 0.009	-
		9	5.025	0	0.025	0.075	2.002± 0.004	-
		10 (POA)	5.1	0	0.1	0	0.006± 0.002	-
7	spruceRH1 (17.05.2022)	1 (POA)	5.4	0	0.1	0	0.022± 0.001	2.91± 0.30
		2	5.3	0	0	0.1	2.003± 0.001	2.85± 0.34
		3	2	3.21	0	0.1	2.003± 0.001	51.90± 0.31
		4	0	5.12	0	0.1	2.003± 0.001	84.27± 0.50
		5	0	5.216	0.096	0.004	0.101± 0.001	82.24± 0.75
		6	2.096	3.21	0.096	0.004	0.105± 0.001	48.19± 0.43
		7	5.396	0	0.096	0.004	0.119± 0.002	2.62± 0.31
		8 (POA)	5.4	0	0.1	0	0.013± 0.001	2.33± 0.31
8	spruceRH2 (18.05.2022)	1 (POA)	5.6	0	0.1	0	0.041± 0.018	1.48± 0.35
		2	5.5	0	0	0.1	2.407± 0.008	1.54± 0.71
		3	2	3.5	0	0.1	2.045± 0.006	54.74± 0.77
		4	0	5.4	0	0.1	2.007± 0.008	85.19± 0.85
		5 (POA)	5.6	0	0.1	0	0.033± 0.004	1.55± 0.29
		6 (POA)	5.6	0	0.1	0	0.032± 0.004	2.10± 0.44
		7	5.596	0	0.096	0.004	0.141± 0.004	1.95± 0.32
		8	0	5.49	0.096	0.004	0.110± 0.005	91.99± 1.09
		9	5.6	0	0.1	0	0.022± 0.004	1.75± 2.79
9	open3 (20.05.2022)	1 (POA)	5.1	0	0.1	0	0.032± 0.004	1.84± 0.46
		2	5	0	0	0.1	2.520± 0.011	1.90± 0.55
		3	5.098	0	0.098	0.002	0.071± 0.004	1.82± 0.40
		4	5.095	0	0.095	0.005	0.150± 0.004	1.81± 0.45
		5	5.09	0	0.09	0.01	0.303± 0.008	1.82± 0.52
9	open4 (21.05.2022)	6 (POA)	5.1	0	0.1	0	0.024± 0.005	1.77± 0.61
		7	5.08	0	0.08	0.02	0.564± 0.003	1.74± 0.53
		8	5.05	0	0.05	0.05	1.340± 0.006	1.68± 0.39
		9	5.02	0	0.02	0.08	2.058± 0.014	1.99± 1.51
		10	0	4.9	0.02	0.08	1.746± 0.009	97.13± 1.05
		11 (POA)	5.1	0	0.1	0	0.028± 0.007	2.02± 0.40

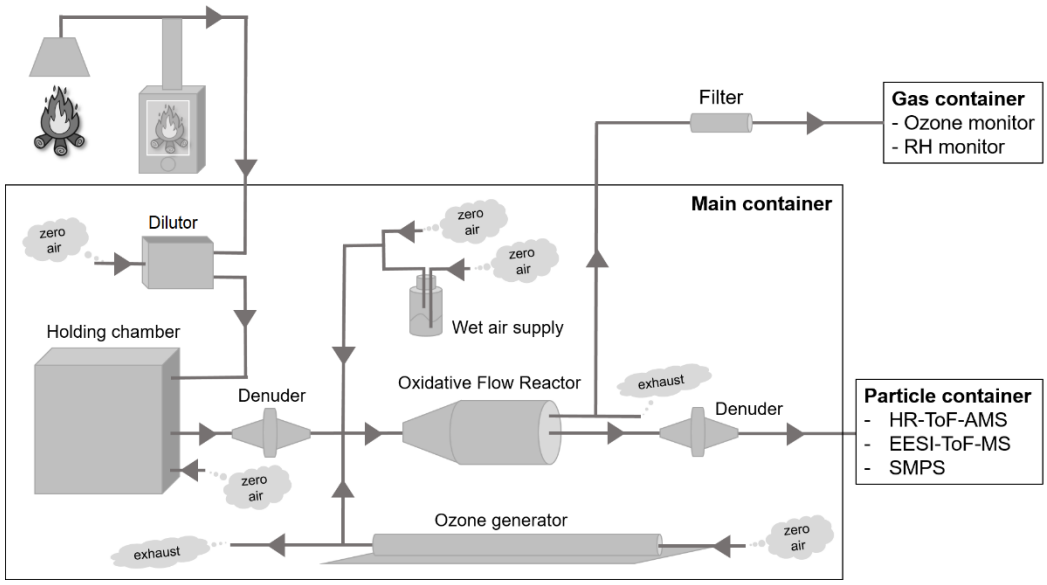

Figure S1: Sketch of the experimental setup in the atmospheric simulation chamber for ozonolysis experiments conducted in the oxidative flow reactor.

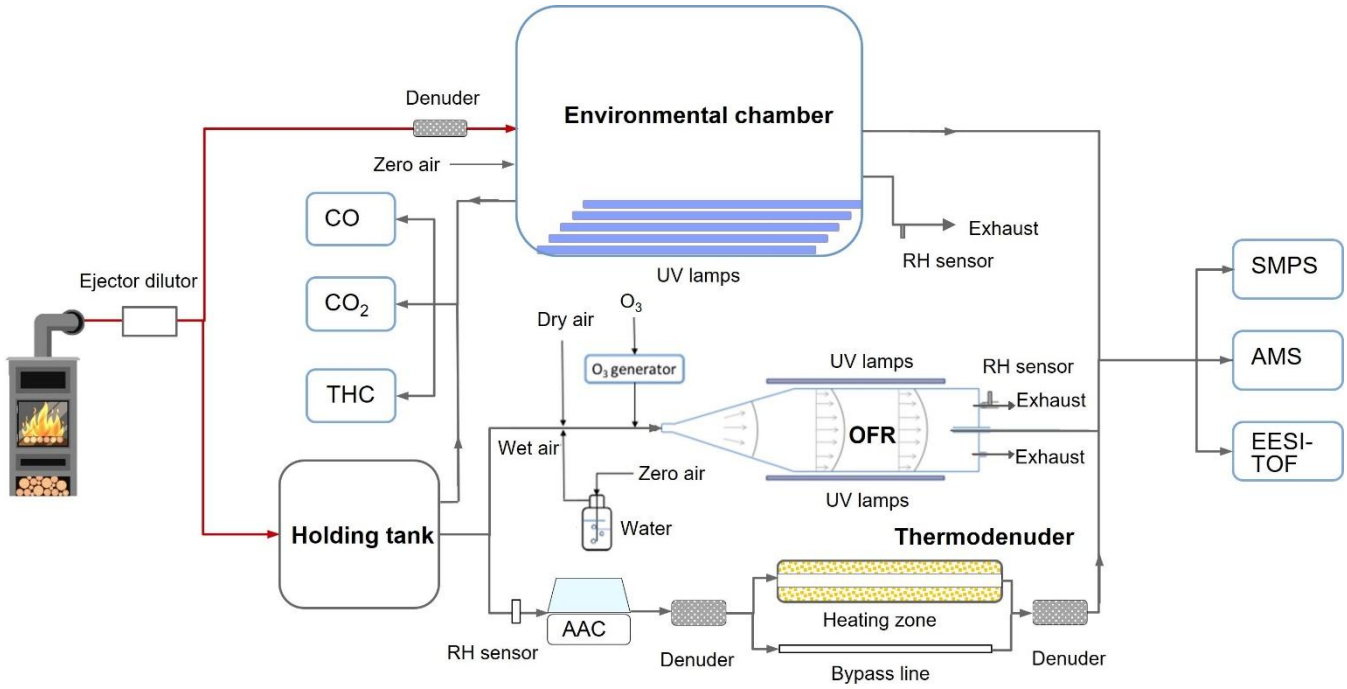

Figure S2: Sketch of the experimental setup in the atmospheric simulation chamber for ozonolysis experiments conducted in the smog chamber.(Adapted from Zhang, 2023; Zhang et al., 2024)

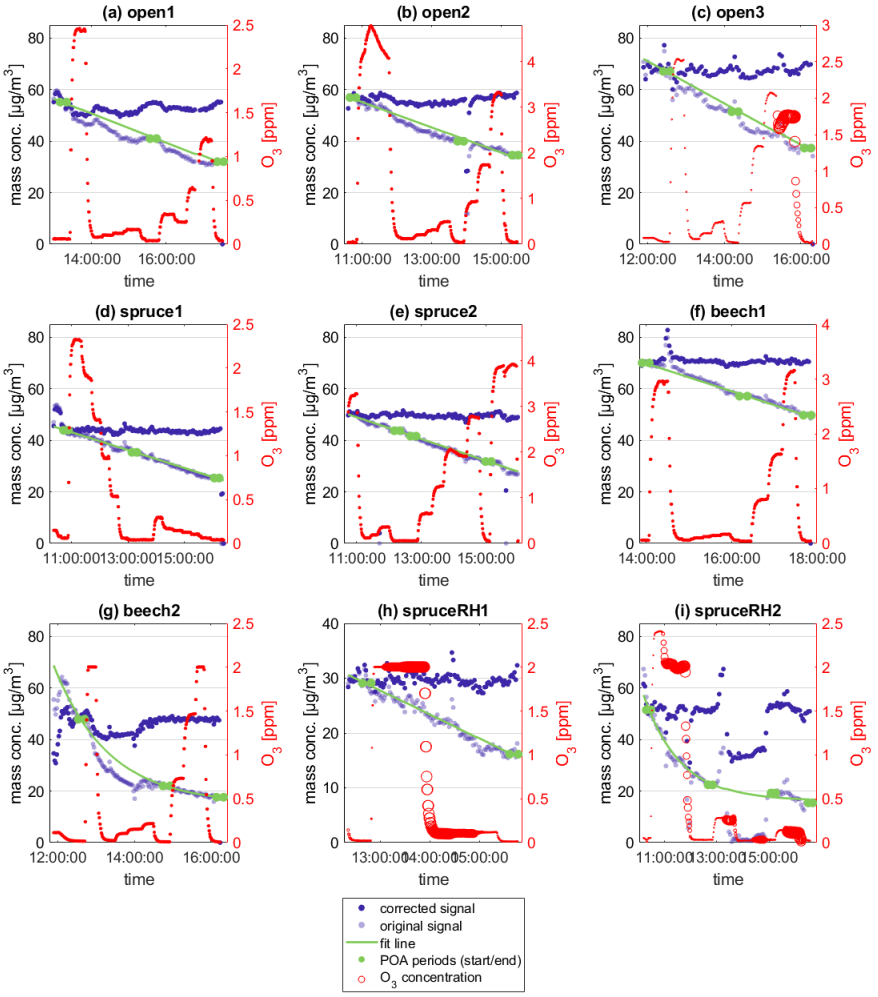

Figure S3: Time series of total organics particle mass concentration as quantified from the HR-AMS analysis for experiments (a)-(i) as given in the subtitle. Each subplot includes the signal as measured on the instrument, and after correction for background decay. For the correction, a fit was determined through periods of measurements at POA conditions; linear fit equation for (a)-(f), (h) y = m*x+c, exponential fit for (g), (i), y = a*exp(b*x)+c. Right y-axis: time series of O_3 concentration. For (c), (h), (i) the size of the marker is a qualitative measure of the relative humidity (RH) level. The bigger the marker size, the higher the RH level (max 97% RH).

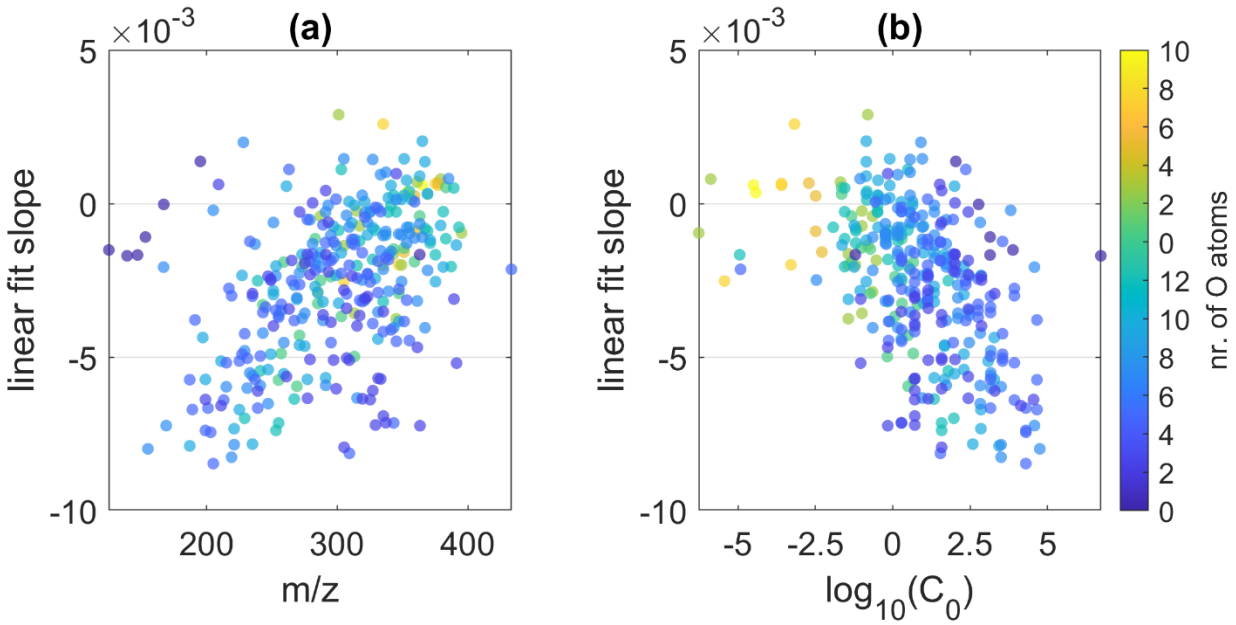

Figure S4: Slopes of linear fit through POA periods to correct for wall losses for ions detected by the EESI from experiment open2 vs (a) m/z ratio and (b) saturation mass concentrations C_0 colored by number of O atoms in the species. C_0 was modelled using a parametrization from Li et al., 2016, $\log_{10}(C_0) = (n^0_C - n_C)*b_C - n_O*b_O - 2*n_C n_O/(n_C+n_O)*b_{CO} - n_N*b_N$, where n^0_C, b_C, b_O, b_{CO}, b_N are constants and n_C, n_O and n_N are the number of C, O and N atoms in each species, respectively. The selection of species was filtered for a threshold of minimum 20 cps during the first POA period and during maximum O_3 exposure. To compare the species' slopes, the fit is based on the relative intensity at each POA period normalized to the first POA period. There is a trend of increasing slopes with increasing m/z and decreasing saturation mass concentrations, i.e. the loss of less volatile species is slower compared to the loss of more volatile species. This observation supports the relevance of particle mass loss driven by partitioning of volatile species out of the particle phase when the gas-phase fraction is absorbed to the walls of sampling lines and holding chamber.

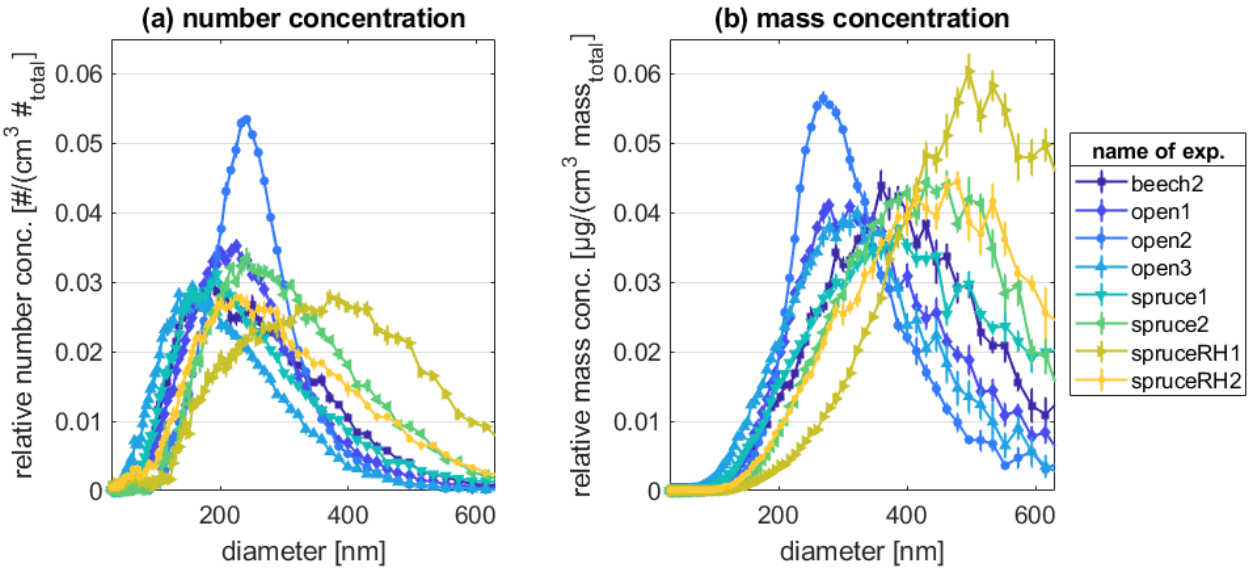

Figure S5: Primary BBOA particle size distribution all experiments (excluding beech), shown as relative (a) number concentration and (b) mass concentration, measured by the SMPS. The first POA period in time is shown. The y scale is relative to the total number or mass of particles measured during the averaged POA period.

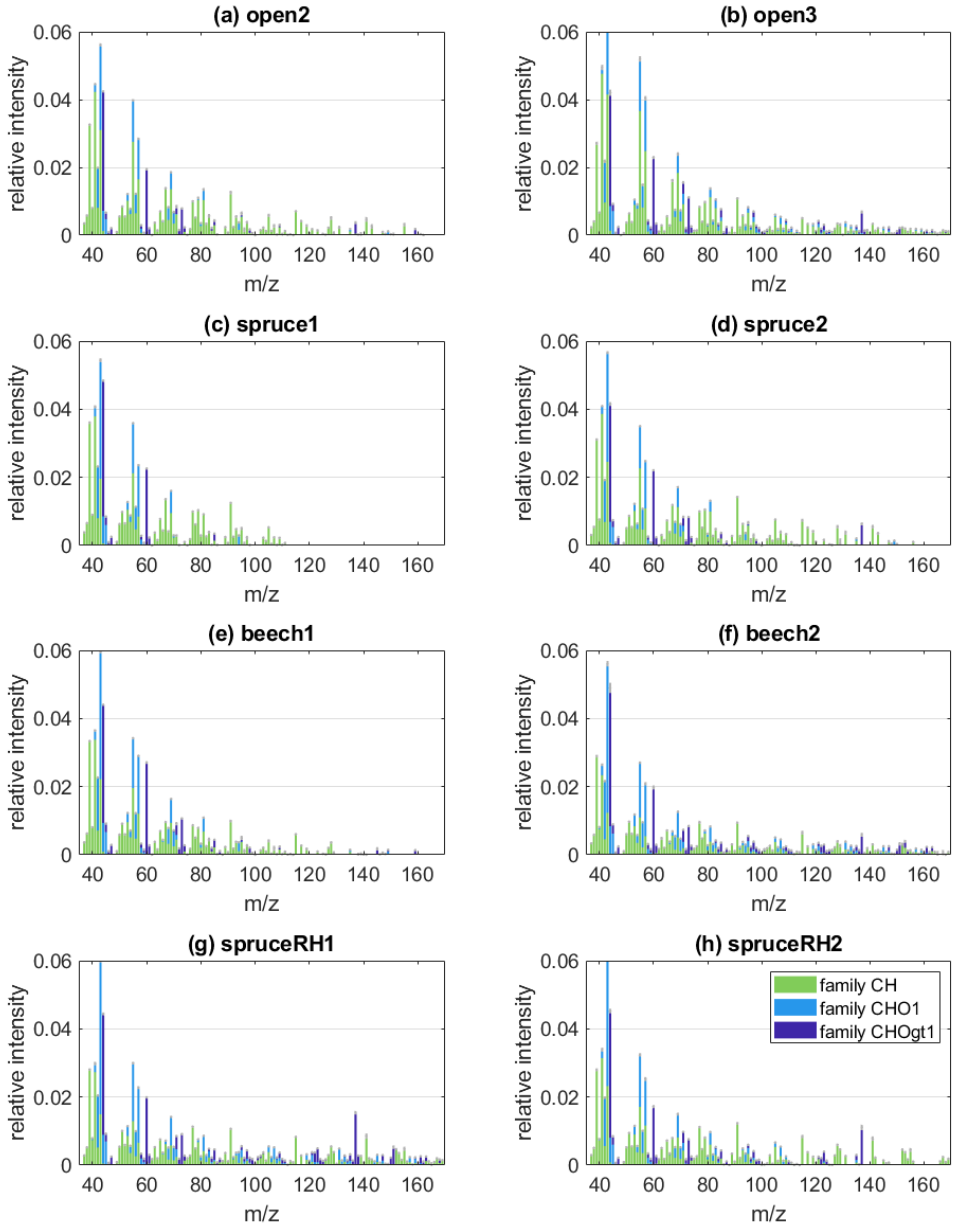

75

Figure S6: AMS mass spectra of all POA conditions scaled with intensity relative to the total average intensity at POA conditions up to m/z 170. The error bars denote the standard error over 10 min of sampling.

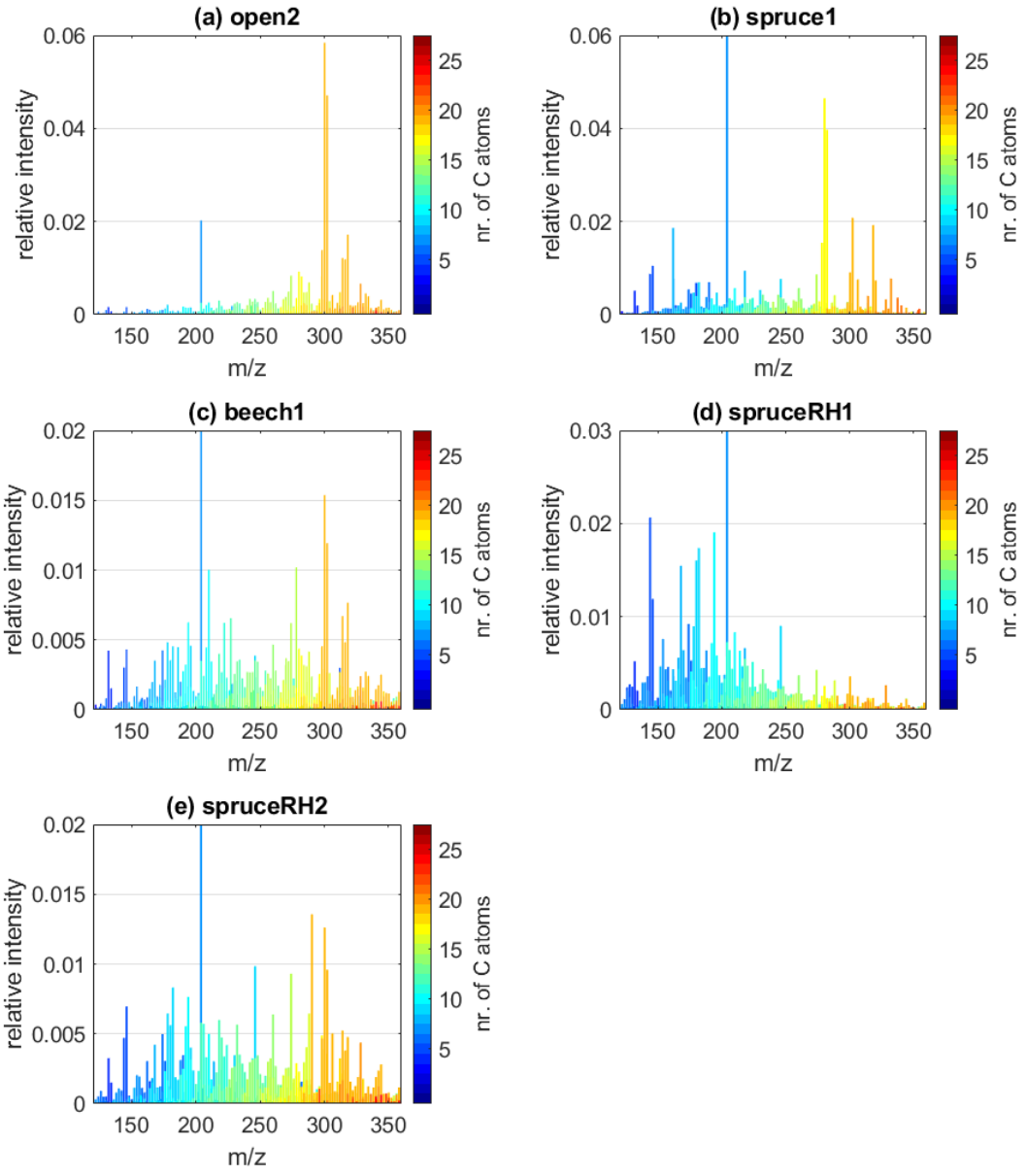

Figure S7: EESI mass spectra at POA conditions scaled with the intensity relative to the total average intensity at POA conditions. As the most intense fraction of $C_6H_{10}O_5$ would expand the y-scale by factor 3 and dominate the intensity distribution over all remaining ions, this ion was removed from the spectrum for clarity. Note that no POA spectra from the experiments spruce and beech2 are included here, as the analysis of the EESI data was not completed due to large instabilities of the electrospray.

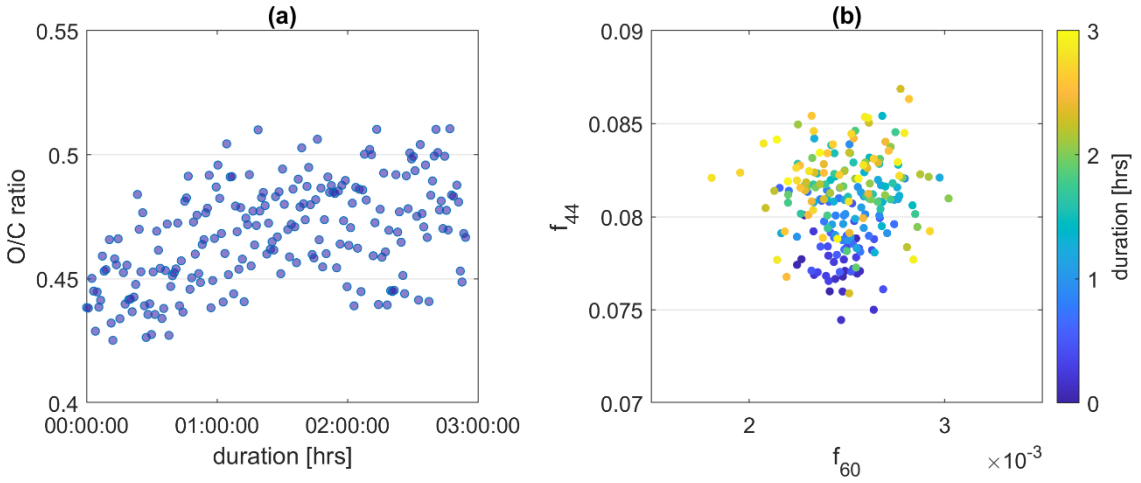

Figure S8: Background control chamber experiment under POA conditions with no O_3 exposure. Evolution of (a) O/C ratio and (b) f_{44} vs f_{60} from AMS analysis within 3 hours of experiment, during which the O/C ratio stayed constant within 10 % of the initial value (averaged over 5 minutes).

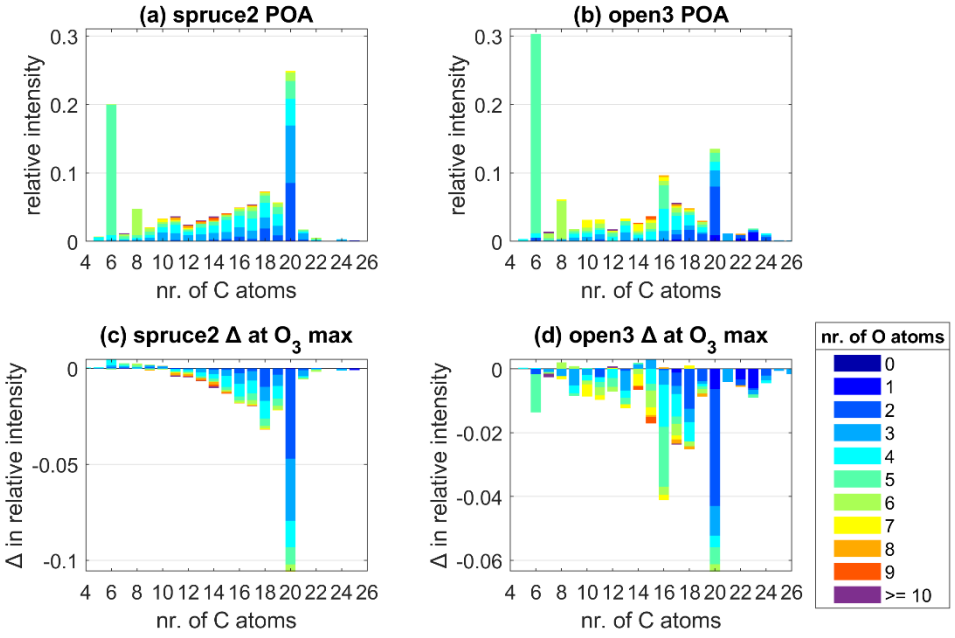

Figure S9 (a)-(b) Average POA composition measured by the EESI scaled as relative intensity compared to total intensity. (c)-(d) Change in relative intensity at highest O_3 exposure of each experiment compared to POA conditions.

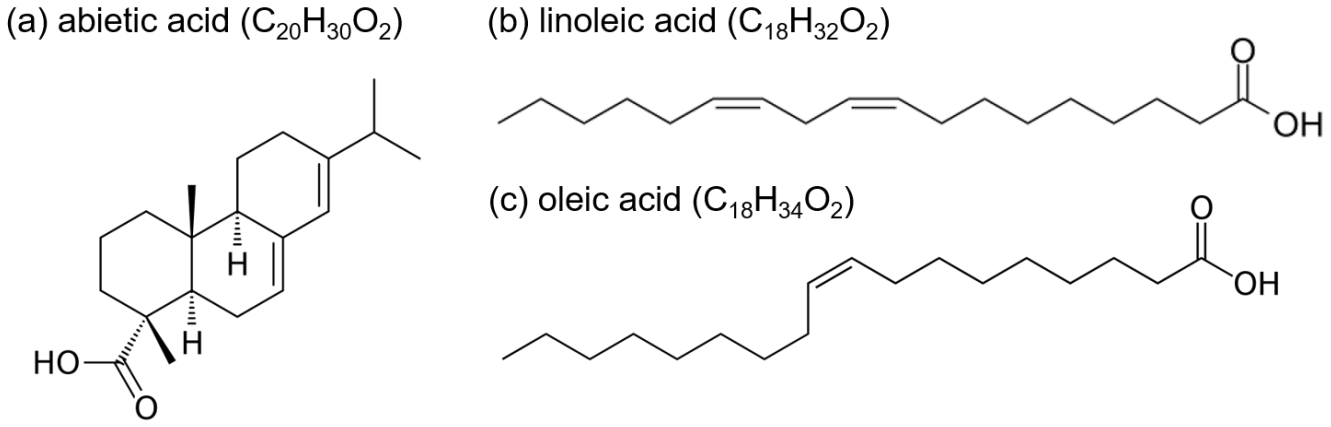

Figure S10: Molecular structures of (a) abietic acid, (b) linoleic acid, and (c) oleic acid. These compounds are possible isomers within the peaks of (a) $C_{20}H_{30}O_2$, (b) $C_{18}H_{32}O_2$, and (c) $C_{18}H_{34}O_2$ that are reactive towards O_3 as detected by the EESI.

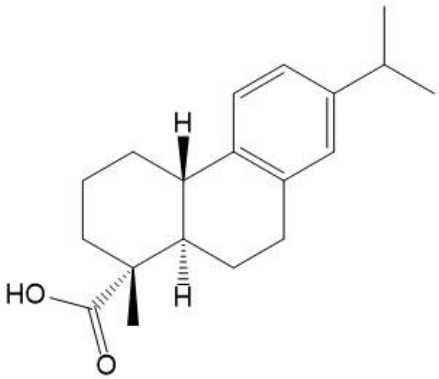

Figure S11: Molecular structure of de-hydroabietic acid. This compound is a possible isomers within the peak of $C_{20}H_{28}O_2$ that is reactive towards O_3 as detected by the EESI. However its reactivity is decreased compared to abietic acid $C_{20}H_{30}O_2$ due to the presence of an aromatic system.

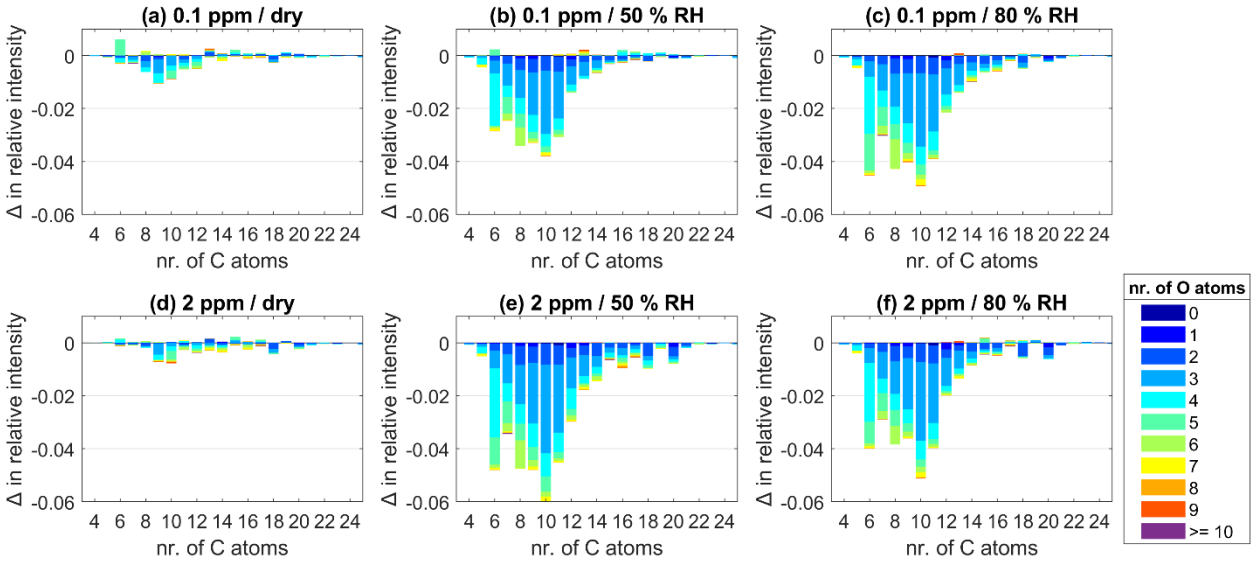

Figure S12: Change in relative intensity compare to POA conditions at 0.1 ppm / 4 ppb hrs O_3 exposure and 2 ppm / 90 ppb hrs O_3 exposure and varying RH as given in the subtitle. This data is from experiment spruceRH1. The exact O_3 and RH conditions are given in Tables S1-S2. The relative intensities are classified by nr. of C atoms and color-coded by nr. of O atoms.

References

Zhang, J.: Bulk and molecular-level composition of primary organic aerosol from wood, straw, cow dung, and plastic burning, 2023.

Zhang, J., Zuend, A., Top, J., Surdu, M., Haddad, I. E., Slowik, J. G., Prevot, A. S. H., and Bell, D. M.: Estimation of the Volatility and Apparent Activity Coefficient of Levoglucosan in Wood-Burning Organic Aerosols, Environmental Science, 2024.